Simulation of x-ray mask defect printability

B. S. Bollepalli[a], S. Hector[b], J. Maldonado[c]

[a]Department of Electrical Engineering, University of Wisconsin-Madison.

[b] Motorola Advanced Products Research Laboratory, Austin, Texas, 78721.

[c] IBM Semiconductor research and development center, Hopewell Junction, NY 12533.

ABSTRACT

The printability of defects in x-ray masks was simulated in three dimensions using the CXrL toolset software developed at the University of Wisconsin and resist dissolution software developed in a collaboration between University of California at Berkeley and Motorola. Isolated defects on x-ray membranes and isolated defects on pellicle membranes mounted behind the x-ray membrane were modeled. Defects in proximity to x-ray absorber features and absorber fabrication defects were also considered. Spheres and parallelepiped defect shapes composed of PMMA, ammonium sulfate, and stainless steel were modeled at exposure gaps in the range 10-50 um.

Attenuation of a variety of potential defect materials was calculated for the IBM Advanced Lithography Facility x-ray source and beam-line x-ray spectrum. The dose-to-clear for 400 and 500 nm thickness APEX-E films was then used to predict what thickness of defect material would result in a printed defect. Image formation model predictions of defect printability in APEX-E resist were compared to attenuation calculations, indicating that defect shape and x-ray phase shift in the defect material has a profound impact on defect printability for materials that are not highly attenuating. Spheres printed more readily than parallelepipeds. Increasing the exposure gap reduced printability slightly.

Experiments to determine the printability of organic spheres added to x-ray masks will be compared to simulation to verify its accuracy. Based on modeling results, the minimum size of isolated defects on x-ray masks that printed will be presented. The minimum size of defects that changed printed line-width will also be discussed. Based on these results, defect inspection sensitivity, cleaning capability, and repair resolution for ¡=175 nm line-width x-ray masks can be established.

Keywords: Defects, Phase-shifting properties, Pellicle defects

1. INTRODUCTION

In proximity x-ray lithography, there is no imaging system and it is 1:1 printing. As a result, the manufacture of high resolution and accurate x-ray masks is critical because a defect present in the mask can translate itself into the printed pattern under suitable printing conditions. The presence of defects in x-ray masks can be mainly attributed to two reasons: due to errors during mask fabrication and due to contamination while using the mask for printing. The contamination of masks in x-ray steppers and growth of particles is described in [Capasso].[1]

Many of the defects can be removed by mask repair [Blauner].[2] However, it is an expensive and laborious work. As a result, a study on the printability conditions for defects in x-ray masks can provide useful information to the mask repair group on what sizes or locations of defects are to be removed. This is precisely the motivation for this study. In [Kluwe][3] a study has been made on the printability conditions for defects in x-ray masks. They obtained some critical defect sizes that would be printed for some special cases. However, our work here is done more elaborately and for a large number of situations. This paper is organized as follows. In section 2, we discuss an abstraction of the various possible defect types and characterize them into different types. In section 3, we discuss the modeling issues of simulation of these defects. Sections 4, 5, 6 and 7 describe the results that we obtained after simulations on Isolated, Interactive and Pellicle type defects. Section 8 deals with the experimental verification. The paper concludes with section 9.

2. Defect types, materials and shapes

Defects can occur anywhere on the x-ray mask. In order to do a study, we classified them to belong to one of the following types: Isolated defects, Interactive defects and Mask fabrication defects which are defined below. **Isolated defects** Defects present in relatively empty areas in the mask are referred to as isolated defects.
Interactive defects Defects present in the vicinity or adjacent to absorber features are referred to as interactive defects.
Mask fabrication defects Defects via the absence of absorber material in some locations or presence of extra absorber material belong to this category.
Pellicle defects The use of a protective covering or pellicle, to make it easier to inspect and clean an x-ray mask has been proposed. in addition, it has been suggested that if a pellicle is on the back side, it may be sufficiently removed so that defects on the pellicle do not print. The presence of foreign materials on this pellicle is referred to as pellicle defects.

There are many possible defect materials that can be found in x-ray masks. since a study of all these materials is difficult, in order to have a qualitative flavor to the study we chose three types of defect materials: inorganic(ammonium sulfate), organic(PMMA) and metallic(stainless steel).

The shape of the defects on x-ray masks is random. For convenience of simulating we considered only two shapes: parallelepiped and spheres. With this we wanted to see if there a particular shape was favored for printability.

3. Modeling and data

For our study, we used Cxrl exposure modeling toolset along with a resist development software called *FastPhoto* described in [Sethian].[4] The ALF spectrum that is shown in Figure 1 is used. The resist material chosen was APEX-E. A constant development time of 90 secs was used with all simulations and the delivered dose varied with the critical dimension. For CDs of 100nm, 125nm and 175nm the delivered doses were 70mJ/cm^2, 70mJ/cm^2 and 75mJ/cm^2 respectively.

4. Isolated defects

4.1. Simulations

For this case we considered two different shapes – a sphere and a parallelepiped. The thickness was varied from $0.1\mu m$ to $5\mu m$ and the mask to wafer gap was varied from $10\mu m$ to $50\mu m$. In order to see the phase shifting properties of the three defect materials, we plotted the fractional absorbance of these materials with thickness and mask to wafer gap. The fractional absorbance of a material is defined as $1 - minimum\ intensity$ point in the aerial image. The exposure time in simulation is chosen such that, in absence of diffractional effects the maximum intensity is at 1.

4.2. Results

The phase shifting properties of the three defect materials are dependent on their size, shape thickness and mask-to-wafer gap. Though we performed simulations for several gaps and sizes of these defects, for conciseness of the paper we provide only some plots. The phase shifting properties of ammonium sulfate parallelepipeds and spheres is shown in figure 8. The first three plots show the fractional absorbance for parallelepipeds with aerial thicknesses of $0.3\mu m$x$0.3\mu m$, $0.5\mu m$x$0.5\mu m$ and $1.0\mu m$x$1.0\mu m$. The last plot shows the phase shifting properties of ammonium sulfate spheres. Figure 9 shows the corresponding data for PMMA and figure 10 corresponds to stainless steel.

In order to study printability we considered a dose of 75mJ/cm^2 and a development time of 90 secs. Table 1 shows the printability of isolated defects with aerial size $0.3\mu m$x$0.3\mu m$ for ammonium sulfate, PMMA and stainless steel. In this table N represents that no defect material is printed, S represents stainless steel, A represents ammonium sulfate and P represents PMMA.

Similarly tables 2 and 3 show the printability for aerial sizes of $0.5\mu m$x$0.5\mu m$ and $1.0\mu m$x$1.0\mu m$.

Table 4 shows the printability of isolated spheres. These figures illustrate that for defects of same volume, spheres have a higher chance of printing as compared to parallelepipeds.
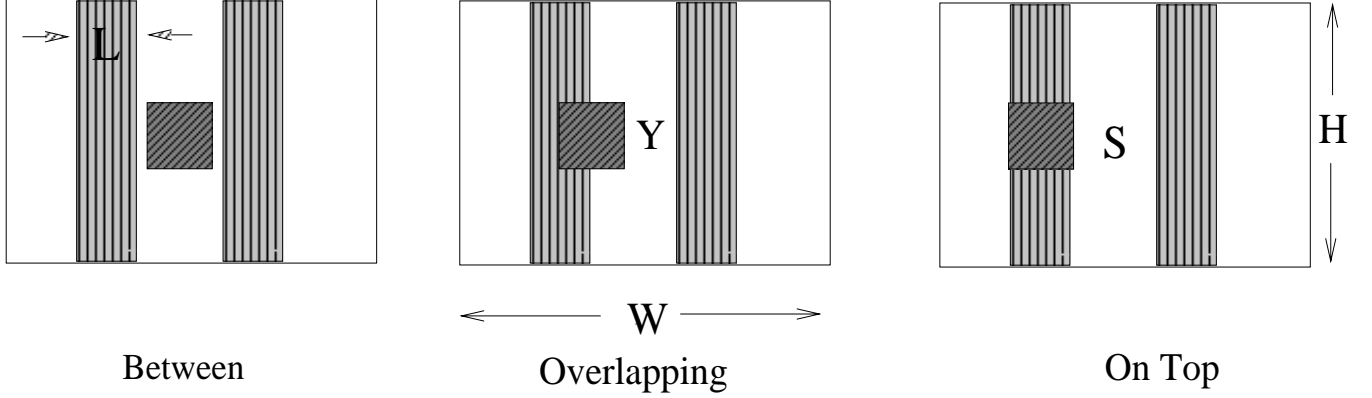
Table 1. Results for isolated defects: printability of 0.3μmx0.3μm squares

Thickness (nm)	10μm gap	15μm gap	20μm gap	25μm gap	40μm gap	50μm gap
100	N	N	N	N	N	N
500	N	N	N	N	N	N
750	S	N	N	N	N	N
1000	S	S	S	S	S	S
3500	S	S	S	S	S	S
4000	A/S	A/S	A/S	A/S	S	S
5000	A/S	A/S	A/S	A/S	S	S

Table 2. Results for isolated defects: printability of 0.5μmx0.5μm squares

Thickness (nm)	10μm gap	15μm gap	20μm gap	25μm gap	40μm gap	50μm gap
100	S	S	S	N	N	N
750	S	S	S	S	N	N
1000	S	S	S	S	S	S
2500	A/S	S	S	S	S	S
3500	A/S	A/S	A/S	A/S	S	S
5000	A/P/S	A/S	A/S	A/S	S	S

Table 3. Results for isolated defects: printability of 1.0μmx1.0μm squares

Thickness (nm)	10μm gap	15μm gap	20μm gap	25μm gap	40μm gap	50μm gap
100	S	S	S	S	S	S
500	A/S	A/S	A/S	A/S	S	S
1000	A/P/S	A/P/S	A/S	A/S	A/S	A/S
1500	A/P/S	A/P/S	A/P/S	A/P/S	A/S	A/S
3500	A/P/S	A/P/S	A/P/S	A/P/S	A/P/S	A/P/S

Table 4. Results for isolated defects: printability of spheres

Diameter (nm)	10μm gap	15μm gap	20μm gap	25μm gap	40μm gap	50μm gap
300	A/P/S	A/P/S	A/P/S	A/P/S	A/P/S	A/P/S
600	A/P/S	A/P/S	A/P/S	A/P/S	A/P/S	A/P/S
1000	A/P/S	A/P/S	A/P/S	A/P/S	A/P/S	A/P/S
2000	A/P/S	A/P/S	A/P/S	A/P/S	A/P/S	A/P/S
5000	A/P/S	A/P/S	A/P/S	A/P/S	A/P/S	A/P/S

Figure 1. Illustration of interactive defects

5. Interactive defects

There are a multitude of possible scenarios for the location of defects near absorber features. We tried to qualitatively describe these using three classes described below. In these three cases we used 1:2 lines and spaces as the mask pattern and three CD's 100nm, 125nm and 175nm.

In Between Defects : Defects lying between the lines of absorber material are termed as in between defects.

Overlapping Defects : defects that grow along the absorber walls and then on to the top of the absorber.

On Top Defects : Defects that sit on top of absorber material, which could be a foreign material contaminating the mask just on the top of part of absorber. This can possibly cause some phase shifting effect.

These three defects are illustrated pictorially in figure 1. The simulations were carried out for $\{L = 100nm, 125nm, 175nm\}$, $\{Y = L, 2L, 4L\}$, $\{T = L, \ldots, 5Y\}$, $\{S = 2L\}$, $\{gap = 10\mu m, \ldots, 40\mu m\}$ and two different absorber materials i.e Au and Ta_4B. Here T represents the thickness of the defect.

5.1. Results

In these simulations, we were primarily interested in seeing how much the line width changes because of the presence of a defect and whether the defect itself is printed or not. We used the rule that if the line-width is changed by more than 10% of the nominal line width then the defect is critical. We noted the minimum size of the defect in each case that caused more than 10% change in line width. Sometimes, the printed lines were very much distorted by the presence of a small defect of size $\approx 0.1\mu$. Figure 4 shows the effect of a typical " in between " type defect. Figure 5 shows it for an " overlapping " defect and figure 6 shows for an " on top " defect. From these we notice that the diffractional effects produced by these types of defects are quite different.

6. Mask fabrication defects

The following figure 2 illustrates mask fabrication defects that we studied. We used a mask containing 1:2 lines and spaces. These defects are mainly due to absence or presence of extra absorber material. The first defect has a gap in the line. the first defect when repaired, is usually filled with a different density material by ion-induced heavy metal deposition. For the purpose of simulation, the filling material we used is gold of density 19.00 g/cm^3.
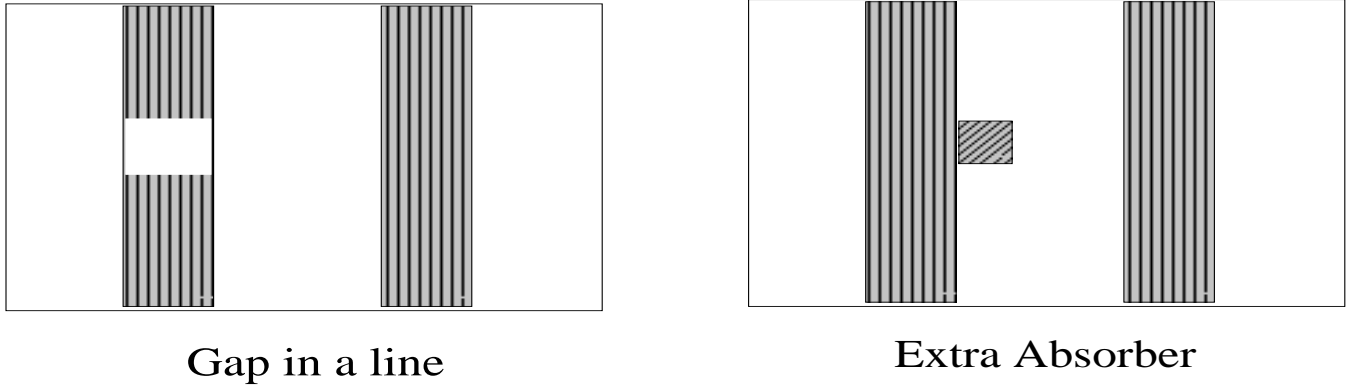
Gap in a line

Extra Absorber

Figure 2. Illustration of mask fabrication defects

Table 5. Results for mask fabrication defects: extra absorber

area (nmXnm)	10μm gap	15μm gap	20μm gap	25μm gap
20X20	89/102	136/138	111/134	139/140
40x40	87/102	134/138	111/134	138/140
60x60	89/127	109/154	96/156	104/154

6.1. Results

6.1.1. Case of extra absorber material

the size of the extra absorber material is varied from 20nmX20nm to 60nmX60nm and we considered 4 different mask-to-wafer gaps. The results for this case are shown in table 5. It lists the minimum and maximum line widths at various gaps. Form this table it is clear that when the defect size is small, large mask-to-wafer gaps tend to correct for the defect and the line width is not changed much.

6.1.2. Case of missing absorber

The size of the gap in one absorber line is varied from 20X20 to 60nmX60nm and again we considered 4 different mask-to-wafer gaps. The results for this case are shown in table 6. From these results we can observe that, increasing the mask-to-wafer gap tends to make the printed line more uniform and has a self correcting behavior. From these results, again we see the corrective tendency of large mask-to-wafer gaps. In this case, at gaps of 25μm though the line was connected there was thickness loss $\approx$ 50 to 100 nm.

Table 6. Results for mask fabrication defects: missing absorber

line-gap nm	10μm gap	15μm gap	20μm gap	25μm gap
20	Broken line	Broken line	Broken line	Connected
40	Broken line	Broken line	Broken line	Connected
60	Broken line	Broken line	Broken line	Broken line

Table 7. Results for mask fabrication defects: different density material

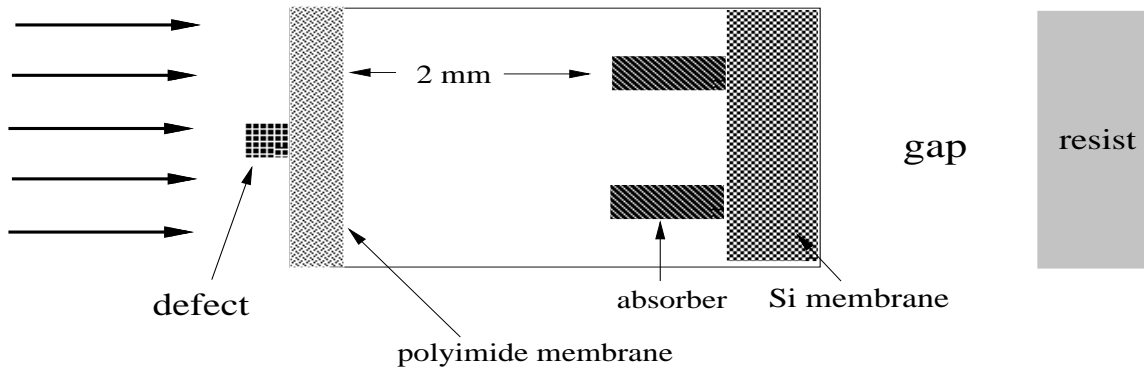| line-gap nm	10μm gap	15μm gap	20μm gap	25μm gap
20	75nm	20nm	0nm	0nm
40	200nm	40nm	0nm	0nm
60	250nm	50nm	0nm	0nm

Figure 3. :Illustration of a pellicle defect

6.1.3. Case of different density material

The results for this case are shown in table 7. The line-widths are within 10% of the nominal line-width. However, there is a thickness loss. This table shows the maximum thickness variation. Again, these results indicate that large gaps can minimize the thickness variation. We used Au with density 18.27g/cm^3 for the absorber features and used Au with density 19.00g/cm^3 for filling.

7. Pellicle defects

To see if a pellicle on the back of the mask can prevent small particles from being printed, we study how the presence of defects on the pellicle effects the printed pattern. The schematic, for this is shown figure 3. Here, we are illustrating the case for back side patterning of the mask which is not practiced at present. We considered varying sizes of defect material to study the printability or effect on the printed pattern.

For the case of isolated pellicle defects, we considered two different defect materials - ammonium sulfate and stainless steel, two different aerial sizes - $0.3\mu m$X$0.3\mu m$X and $1.0\mu m$X$1.0\mu m$ and several pellicle gaps and defect thicknesses. For the case when the defect shape is a sphere, we considered only one material - stainless steel. The results indicated that for defect sizes less than $1.0\mu m$X$1.0\mu m$ in aerial size, a pellicle gap of 1mm is enough to avoid its printability.

For the case of interactive pellicle defects, figure 8 shows printed lines for a 1:1 lines and spaces pattern, with a pellicle defect of size $0.2\mu m$X$0.2\mu m$X$0.7\mu m$ and a pellicle gap of 7mm. In this case we see a bending of lines and there is a lens like behavior. This also indicates that interactive pellicle defects severely effect the printed pattern.

8. Experimental Verification

9. Conclusions

The conclusions of this work are several fold. For the sake of convenience, we have split these into various defect categories.

9.1. Isolated

We note from figures 7 through 9 that the fractional absorbance is greatly increased due to phase shifting. The printability simulations showed that the geometrical shape is critical for printability - small spheres print more easily than parallelepipeds. One common trend in printability is that it increases with aerial size and decreases with gap. From the simulations, the critical sizes for printability of isolated defects are:

ammonium sulfate : 0.3x0.3x4.0 μm.

PMMA : 0.5x0.5x5.0 μm.

stainless steel : 0.3x0.3x0.7 μm.

and in the case of spheres the minimum size to look for is 0.2μm in diameter.

9.2. Interactive

For conciseness of the paper we could not show the data obtained in simulations on interactive defects. We observed that, even small defects of thickness $\approx 0.1\mu$m altered the line width by more than 10%. This data also indicated that " in between " type defects are the worst among the three types we studied, as they caused the largest line width change and sometimes the defects themselves were printed. For "on top" type defects, the line width variation was quite less. However, they produced a thickness loss because of Poisson spots produced by diffraction effects. Both the "overlapping" and "on top" defect types had minimal effect on the line width of the neighboring line.

9.3. Mask Fabrication

One main observation is that, in all the mask fabrication defects a large gap helps in correcting for the defects. For the case of missing absorber, if the gap is $\approx$ 10nm or less, the printed line is uniform. This suggests that small gaps in lines can be ignored without repair. For the case, when we fill gaps in lines by ion induced deposition of material of different density, there is a thickness variation in the printed line. however, it disappears at large gaps.

9.4. Pellicle defects

Printability of isolated pellicle defects increases with aerial size and decreases with pellicle gap. this behavior is similar to that of the isolated mask defects. Some critical sizes and pellicle distance pairs are

$\approx 0.3\mu$mX0.3μm at 1mm pellicle distance and

$\approx 1.0\mu$mX1.0μm at 1cm pellicle distance.

Contrary to the isolated pellicle defects, the printability of pellicle defects increases in the presence of absorber features. We do not notice it in the isolated case because we are observing intensities at the resist in which we are not considering phase. However, in the interaction case, the incoming plane waves are altered severely by the pellicle defects and the mask does not see a plane wave anymore. To loosely say, it is some what spherical and as a result the printed pattern is drastically altered. In some cases, we see the bending of lines and this is like a lens behavior. In order to avoid the effects of the pellicle defects, we feel that large pellicle distances are necessary $\approx$ 2 cm.

9.5. Experimental studies

REFERENCES

1. C. Capasso, "X-ray induced mask contamination and particulate monitoring in x-ray steppers," *Electron, Ion and Photon beam Conference, Atlanta, June* **1**, pp. 1–10, 1996.
2. P. G. Blauner and J. Mauer, "X-ray mask repair," *IBM J. RES¿ DEVELOP.* **37 No. 3**, pp. 421–434, 1993.
3. T. S. A. Kluwe, H. Lutzke and K. H. Muller, "Printability of x-ray mask defects at various printing conditions and critical dimensions," *J. Vac. Sci. Technol. B* **8(6)**, pp. 1609–1613, 1990.
4. J. Sethian, "A fast marching level set method for monotonically advancing fronts," *Centre for Pure & Applied Mathematics, UC Berkeley, report PAM-652* **-**, pp. –, -.